Strathprints Institutional Repository

CrossMark

Does anisotropy promote spatial uniformity of stent-delivered drug distribution in arterial tissue?

Sean McGinty [a,*], Marcus Wheel [b], Sean McKee [a], Christopher McCormick [c]

[a] Department of Mathematics and Statistics, University of Strathclyde, Glasgow, UK
[b] Department of Mechanical and Aerospace Engineering, University of Strathclyde, Glasgow, UK
[c] Department of Biomedical Engineering, University of Strathclyde, Glasgow, UK

ABSTRACT

In this article we investigate the role of anisotropic diffusion on the resulting arterial wall drug distribution following stent-based delivery. The arterial wall is known to exhibit anisotropic diffusive properties, yet many authors neglect this, and it is unclear what effect this simplification has on the resulting arterial wall drug concentrations. Firstly, we explore the justification for neglecting the curvature of the cylindrical arterial wall in favour of using a Cartesian coordinate system. We then proceed to consider three separate transport regimes (convection dominated, diffusion dominated, reaction dominated) based on the range of parameter values available in the literature. By comparing the results of a simple one-dimensional model with those of a fully three-dimensional numerical model, we demonstrate, perhaps surprisingly, that the anisotropic diffusion can promote the spatial uniformity of drug concentrations, and furthermore, that the simple analytical one-dimensional model is an excellent predictor of the three-dimensional numerical results. However, the level of uniformity and the time taken to reach a uniform concentration profile depends on the particular regime considered. Furthermore, the more uniform the profile, the better the agreement between the one-dimensional and three-dimensional models. We discuss the potential implications in clinical practice and in stent design.

1. Introduction

Local drug delivery to the arterial wall is becoming an increasingly common method of tackling restenosis (re-narrowing of the lumen) following percutaneous coronary interventions (PCIs). These PCIs, commonly known as angioplasty, are non-surgical procedures used to treat narrowed arteries as a result of coronary heart disease (CHD). The most common of these PCIs is the insertion of a small mesh-like device called a stent [1], to act as a scaffold and widen the lumen. Some of the methods of reducing restenosis include directly coating the stent with a drug (the so-called drug-eluting stent) and, more recently, by inflating a drug-coated balloon at the required site [2,3]. Modelling the transport of drug from the device through the arterial wall is extremely challenging given the multitude of factors that influence drug distribution. For example, a portion of drug will likely be carried away by the pulsatile flowing blood in the lumen and the

drug that enters the arterial wall is subject to diffusion, convection and binding, while at the same time the artery is under the influence of contraction and relaxation. To complicate matters further, the arterial wall is a heterogeneous structure, consisting of three distinct layers with possibly different anisotropic properties in each layer. Notwithstanding, many models of differing dimensionality and different simplifying assumptions have been proposed for modelling the transport through these tissue layers. These models have emanated from the substantial body of work on mass transport in biological tissue which has featured heavily in the literature over the past few decades. We refer the interested reader to the review by Khaled and Vafai [4] for background reading and to the recent work by the same group [5] on mass transport in mammary glands which is an excellent exemplar of a different application of mass transport in biological tissue.

Whilst some authors explicitly account for the curvature of the arterial wall (see e.g. [3]), in the literature it is standard to neglect the curvature so that the resulting model may be written in a Cartesian coordinate framework (see e.g. [6–8]). However, this assumption is never justified mathematically. Tzafriri et al. [7] did, however, state that they had carried out numerical simulations

Nomenclature

a	arterial inner radius	x	Cartesian spatial coordinate
b	arterial outer radius	X	non-dimensional spatial coordinate
c	volume averaged drug concentration	y	Cartesian spatial coordinate
c_0	initial stent drug concentration	Y	non-dimensional spatial coordinate
D	radial diffusion coefficient	z	Cartesian/cylindrical spatial coordinate
D_1	axial/circumferential diffusion coefficient	Z	non-dimensional spatial coordinate
Da_1	non-dimensional first Damkohler number	α	ratio of arterial wall thickness to half-strut separation
Da_2	non-dimensional second Damkohler number	γ	ratio of radial to axial diffusion coefficient
K	drug absorption rate	Γ	computational domain
L	arterial wall thickness	Γ_1	drug containing region of abluminal facing plane
L_1	half strut separation	Γ_2	drug containing region of abluminal facing plane
L_2	half strut thickness	Γ_3	drug-free region of abluminal facing plane
r	cylindrical radial coordinate	ϵ	ratio of arterial wall thickness to arterial radius
Pe	non-dimensional Peclet number	θ	cylindrical circumferential coordinate
R	reaction term	$\theta^\star$	wedge angle with abluminal-facing arc length equal to the half strut separation
t	time		
T	non-dimensional time	λ	drug release rate
v	magnitude of transmural velocity		

which illustrated that maximal tissue drug content was 10% lower when neglecting the curvature dependent term. However, this was for a specific set of parameter values. Another common simplification is to treat the arterial wall as a single layer with uni-directional convection and isotropic diffusion properties (see [7,9–12] among others). Coupled with the negligible curvature assumption, this allows the transport equation in the arterial wall to be written in one-dimension as

$$\frac{\partial C}{\partial t} + v\frac{\partial C}{\partial x} = D\frac{\partial^2 C}{\partial x^2} - R, \qquad (1.1)$$

where C is the volume-averaged concentration of drug in the arterial wall, v is the magnitude of the transmural convection, D is the diffusion coefficient of drug within the tissue and R is some reaction term to account for the effects of binding. A variety of models for R have been reported (see [1] for a review of these). However, there exists experimental evidence that within each layer anisotropy may be important. For example, diffusion within the tissue has been reported to be anisotropic [13,14] with the diffusion coefficient in the radial direction at least 10 times (and possibly as much as 100 or 1000 times) less than that in the circumferential and axial directions. This anisotropy cannot be captured by a one-dimensional model and it is unclear the effect this simplification has on the resulting concentration profiles.

Realising this, many authors have turned to higher dimensional models. For example, [15,8] both considered a two-dimensional model in a Cartesian geometry, and [16] proposed a two-dimensional model in a cylindrical co-ordinate system. The focus of the work in [15] was on the difference in the transport properties of two commercially available drugs (paclitaxel and sirolimus) and how this can affect the distribution of drug in the arterial wall, while [16] focussed on the influence of strut compression on the drug transport properties of the arterial wall. Zhu et al. [8], on the other hand, were more concerned with the effect of diffusion (in their two-dimensional model) on the resulting arterial wall drug levels. In each case, anisotropic diffusion coefficients were accounted for, with the diffusion coefficient in the radial direction chosen to be different from that in the circumferential direction. Being two-dimensional, these models were unable to study the effect of a different diffusion coefficient in each of the three mutually perpendicular directions.

Weiler et al. [17] provided a broad generalization of the works of [18–20]: a three-dimensional model of drug transport in the lumen and the arterial wall. However, only the steady diffusion equation (no time-dependence, convection nor reaction) was considered in the arterial wall and drug diffusion was assumed to be isotropic. Horner et al. [21] appear to be one of the first groups to provide a three-dimensional reaction–diffusion–convection model in a realistic geometry (obtained using ABAQUS software). Whilst having the advantage of allowing for a variation in the diffusion coefficient in three spatial directions, the authors only considered the case in which the axial and circumferential diffusion coefficients were the same. They also make a number of significant simplifications. Perhaps the most unrealistic assumption is that of a constant drug source: the drug concentration on the stent remains constant and does not deplete.

Whilst not explicitly considering anisotropic diffusion, Saylor et al. [22] most recently attempted to better account for the structure of the arterial wall by presenting a structure-sensitive continuum model of arterial drug deposition. Their model attempts to account explicitly for variations in tissue structure, and they are able to derive a closed form analytical solution of their one-dimensional model, after making some simplifying assumptions. Using their analytical expression, they fit for the unknown material parameters in the model based on ex-vivo experimental data, and they found that the data were well fit by the model.

In this paper, we investigate the role of anisotropic diffusion on the resulting arterial wall drug distribution following stent-based delivery. We start by exploring the justification for neglecting the arterial curvature before investigating the impact of the transport regime (convection dominated, diffusion dominated, reaction dominated) on the uniformity of drug concentrations in the abluminal-facing plane. In this context, the word "uniformity" should be interpreted loosely as the closeness of the numerical drug concentration values in the abluminal-facing plane: the more uniform the drug concentrations are, then the closer their difference is to zero. We then proceed to compare drug concentrations obtained from a one-dimensional model with those from the corresponding three-dimensional anisotropic model. Analytical solutions are derived for the one-dimensional model and the open source computational software openFoam is utilised to compute the three dimensional solution. We conclude by providing recommendations for when a one-dimensional model may reasonably be used and, further, we comment on stent design (in terms of strut thickness and strut spacing) based on our findings and desired clinical outcome.

2. The mathematical models

Before setting down the models, we specify the simplifying assumptions that are to be made. Firstly, since the focus of this research is to investigate the effect of anisotropic diffusion on drug distribution in the tissue, we do not model the release of drug from the device. Instead, we assume that the drug concentration at the boundary between the lumen and the arterial wall may be described by an exponentially decaying function of time [24,25]. Secondly, we impose zero-flux conditions on the lumen/tissue interface and zero concentration on the exterior of the arterial wall. In the in vivo scenario, Robin type conditions are likely to be more appropriate in both cases: a fraction of drug will be washed away by the blood flow; and, while the drug concentration at the exterior of the tissue may be small, it is unlikely to be identically zero. However, the drug lost to the blood could be accounted for in the exponentially decaying boundary condition at the lumen, and all of the boundary conditions assumed here may, in principle, be maintained in ex-vivo experiments. Thirdly, we assume as is standard in the literature, that convection is uni-directional and acts radially due to the pressure difference across the arterial wall. We make the further reasonable and common assumption that the diffusion coefficients and reaction parameters in the arterial wall are independent of space, concentration and time.

Stent manufacturers are predominantly concerned with the mechanical integrity of the device and as such the stent design is usually the first consideration. The stent must be flexible and expandable and stay in situ after deployment. During the expansion process the stent should undergo minimum shortening and after implantation should conform to the natural geometry of the vessel without any unnatural straightening. Circumferential strength is another key component; without this, the stent will collapse under the strain of the artery. A wide variety of stent designs are currently available and despite their sometimes complex appearance, they are designed to have a regular structure. If the stent is 'flattened out' (or 'unwrapped') then there is usually a clear repeating 'unit cell'. These unit cells are separated by connectors to enhance the flexibility and conformability. For the purposes of this paper, we consider an idealised stent geometry exhibiting equally spaced struts and a regular structure, with the unit cell taking the form of a square (see Fig. 1 for a portion of the stent). In many currently available stents, the unit cell takes the form of a diamond, from which our unit cell can be seen to be a special case.
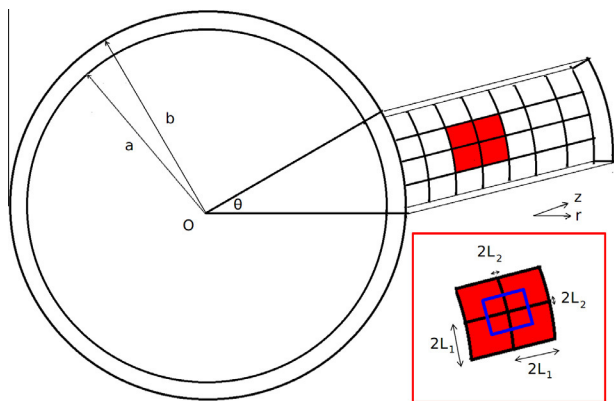

Fig. 1. Schematic showing the geometry of the problem. The inner radius is denoted by a while the outer radius is denoted by b. The arterial wall is represented by $b - a$. We need only consider a portion of this domain, where θ controls the number of struts to be included in the computation. The strut separation is denoted $2L_1$ while the strut thickness is $2L_2$. In practice our computational domain comprises one quarter of the region bounded by the blue box and we apply zero flux conditions along the lines of symmetry.

Now, consider a drug-eluting stent with idealized strut geometry as displayed in Fig. 1. When placed inside the artery, we assume that the struts impinge upon (but do not penetrate into) arterial tissue. Because of the symmetry of the problem, we need only consider a portion of the cylinder, a wedge, as shown in Fig. 1. Now consider the typical section shaded red in Fig. 1. It is readily seen that our computational domain need only comprise one quarter of the region bounded by the blue box, with zero flux conditions being applied along the lines of symmetry. This significantly reduces the computational burden.

2.1. Justification for using a Cartesian system

The equation of drug transport in the arterial wall is stated in a cylindrical co-ordinate system as:

$$\frac{\partial c}{\partial t} + v\frac{\partial c}{\partial r} = D\left(\frac{\partial^2 c}{\partial r^2} + \frac{1}{r}\frac{\partial c}{\partial r}\right) + D_1\left(\frac{1}{r^2}\frac{\partial^2 c}{\partial \theta^2} + \frac{\partial^2 c}{\partial z^2}\right) - Kc,$$
$$a < r < b, \quad 0 < \theta < \theta^\star, \quad 0 < z < L_1, \tag{2.1}$$

where $c = c(r, \theta, z, t)$ is the volume averaged concentration of drug in the tissue of thickness $(b - a)$ and the parameters v and K represent the magnitude of the transmural velocity and the absorption rate of drug within the system (for example to smooth muscle cells, interstitial tissue or through *vasa vasorum* sinks). We assume that the diffusion coefficient of the drug in the radial direction, D, is different from that in the circumferential and axial directions, D_1. The parameter L_1 is the half strut separation as shown in Fig. 1 and $\theta^\star$ is the angle of the wedge which gives rise to an abluminal-facing arc length of L_1. Let us introduce the non-dimensional variables

$$T = Dt/(b-a)^2, \quad X = (r-a)/(b-a), \quad C = c/c_0,$$
$$Y = \theta/\theta^\star, \quad Z = z/L_1,$$

where c_0 is the initial drug concentration on the stent. Then (2.1) becomes

$$\frac{\partial C}{\partial T} + Pe\frac{\partial C}{\partial X} = \frac{\partial^2 C}{\partial X^2} + \frac{\epsilon}{1+\epsilon X}\frac{\partial C}{\partial X} + \frac{1}{\theta^{\star 2}\gamma}\left(\frac{\epsilon}{1+\epsilon X}\right)^2\frac{\partial^2 C}{\partial Y^2} + \frac{\alpha^2}{\gamma}\frac{\partial^2 C}{\partial Z^2}$$
$$- Da_2 C, \quad 0 < X < 1, \ 0 < Y < 1, \ 0 < Z < 1, \tag{2.2}$$

where $Pe = v(b-a)/D$ and $Da_2 = K(b-a)^2/D$ are the Peclet number and second Damkohler number, respectively, and

$$\gamma = D/D_1, \quad \epsilon = (b-a)/a \quad \text{and} \quad \alpha = (b-a)/L_1.$$

We note that ϵ, the ratio of arterial wall thickness to arterial radius, is typically small. Thus we may write

$$\frac{\epsilon}{1+\epsilon X} = \mathcal{O}(\epsilon).$$

Furthermore, by trigonometric arguments, for $\theta^\star$ small, $\theta^\star \approx L_1/a$. Taking these together, the factor multiplying the second derivative with respect to Y can be approximated by

$$\frac{1}{\theta^{\star 2}\gamma}\left(\frac{\epsilon}{1+\epsilon X}\right)^2 \approx \frac{\alpha^2}{\gamma}.$$

Thus we may write (2.2) as

$$\frac{\partial C}{\partial T} + Pe\frac{\partial C}{\partial X} \approx \frac{\partial^2 C}{\partial X^2} + \epsilon\frac{\partial C}{\partial X} + \frac{\alpha^2}{\gamma}\left(\frac{\partial^2 C}{\partial Y^2} + \frac{\partial^2 C}{\partial Z^2}\right) - Da_2 C,$$
$$0 < X < 1, \ 0 < Y < 1, \ 0 < Z < 1. \tag{2.3}$$

It is now evident that if $\epsilon \ll 1$ and $\epsilon \ll \alpha^2/\gamma$, then the term which arises as a result of the cylindrical coordinate system is negligible and we may write

$$\frac{\partial C}{\partial T} + Pe \frac{\partial C}{\partial X} \approx \frac{\partial^2 C}{\partial X^2} + \frac{\alpha^2}{\gamma} \left(\frac{\partial^2 C}{\partial Y^2} + \frac{\partial^2 C}{\partial Z^2} \right) - Da_2 C,$$
$$0 < X < 1, \ 0 < Y < 1, \ 0 < Z < 1, \tag{2.4}$$

which is essentially the equation for transport in a rectangular co-ordinate system. In addition, if $Pe \ll 1$ then the convection term is negligible compared with diffusion and, further, if $Da_2 \ll 1$ then the reaction term is also negligible in comparison with diffusion. Now, for the system under consideration in this paper, we have that $\epsilon = 0.1$ and $\alpha^2/\gamma = 2.0$ (see Table 1) and so it is reasonable to approximate the curved arterial wall geometry as rectangular. We note that several authors have developed one-dimensional models which consider drug transport only in the radial direction and neglect the curvature of the arterial wall, allowing them to utilize a Cartesian co-ordinate system. For the one-dimensional case we see immediately from (2.3) that approximating the cylindrical geometry as rectangular is justified provided that $\epsilon \ll 1$.

2.2. Parameter values

For this study we estimated the parameter values based on data currently available in the literature. In line with the findings by [14] we assume that the radial diffusion coefficient is at least ten times smaller than the circumferential and axial diffusion coefficients and consider a range of values based on [7,15], which satisfy this condition. The thickness of the tissue and arterial radius are chosen to be in line with those of a porcine coronary artery [7] which is the most widely used model due to its anatomical similarity to the human coronary artery. The magnitude of the transmural velocity is generally considered to be in the range $10^{-8} - 10^{-7}$ ms^{-1} [7,10]. We choose the stent strut thickness and separation based on the works of [15]. A representative drug release rate of 10^{-5} s^{-1} is selected [24,25]. Finally, we consider a range of drug absorption rates covering two orders of magnitude [21,23]. The values considered are summarised in Table 1.

Many of these parameters are in fact drug-dependent. For example, the drug diffusion coefficient in the tissue varies depending on the particular molecule in question and the drug release rate may be highly dependent on the diffusion of drug within the stent coating, if indeed the drug is contained within a coating. Furthermore, the drug absorption rate (and indeed the binding model) will depend on the binding properties of the particular drug within the tissue. We note that there is a large degree of uncertainty in the values reported in the literature. Often these values have been estimated based on experiments with a small number of repetitions, and in some cases effective diffusion coefficients (which inherently include such effects as transmural convection and binding) are calculated. Furthermore, the transport properties vary from species to species and may well vary substantially between tissue samples of the same species. Since we are lacking a full set of our model parameters for the drugs commonly coated on drug-eluting stents, we are not able to run drug-specific simulations. However, we do make some comments on specific drugs in Section 5. The values reported here should be treated as indicative only and could easily be an order of magnitude higher or lower in reality. With this in mind, a range of values are considered.

2.3. Three dimensional model

We proceed to solve the three dimensional diffusion–convection–reaction equation in a rectangular geometry. Without loss of generality, we solve over the radial region $x \in (0, L)$ (where $L = b - a$) rather than $x \in (a, b)$. The computational domain, Γ, is displayed in Fig. 2.

Let us define the following drug-containing regions:

$$\Gamma_1 := \{ x = 0, \ 0 \leqslant y \leqslant L_1, \ 0 \leqslant z \leqslant L_2 \}$$
$$\Gamma_2 := \{ x = 0, \ 0 \leqslant y \leqslant L_2, \ L_2 < z \leqslant L_1 \}.$$

We denote the initially drug-free region of the $y-z$ plane in contact with the lumen by Γ_3, where

$$\Gamma_3 := \{ x = 0, \ L_2 \leqslant y \leqslant L_1, \ L_2 \leqslant z \leqslant L_1 \}.$$

Then, denoting the volume averaged drug concentration by $c(x, y, z, t)$ and the stent drug decay rate by λ, we may write the model as

Table 1
Table of parameter values.

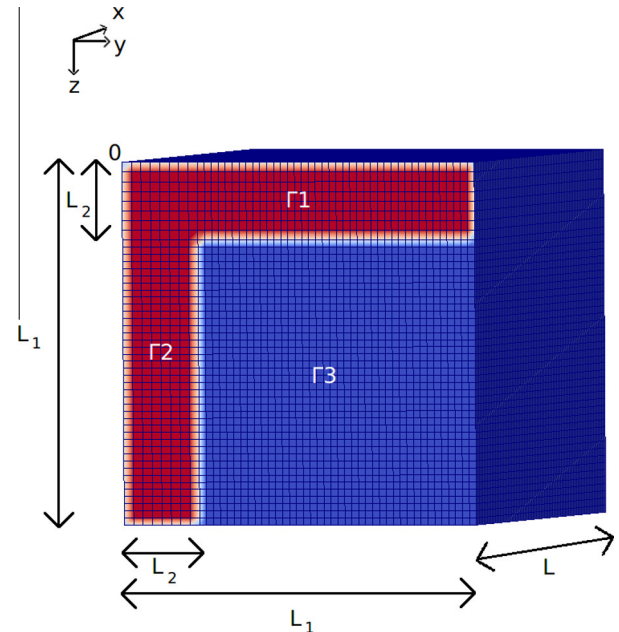| Parameter	Symbol	Value	References
Arterial inner radius	a	5×10^{-3} m	[7]
Arterial outer radius	b	5.5×10^{-3} m	[7]
Arterial wall thickness	L	5×10^{-4} m	[7]
Axial and circumferential diffusion coefficient	D_1	$10^{-11} - 10^{-10}$ m^2 s^{-1}	[7,15]
radial diffusion coefficient	D	$10^{-12} - 10^{-11}$ m^2 s^{-1}	[7,15]
Half strut separation	L_1	3.5×10^{-4} m	[15]
Half strut thickness	L_2	7.5×10^{-5} m	[15]
Magnitude of transmural velocity	v	$10^{-8} - 10^{-7}$ m s^{-1}	[7,10]
Drug absorption rate	K	$10^{-5} - 10^{-4}$ s^{-1}	[21,23]
Drug release rate	λ	10^{-5} s^{-1}	[24,25]

Fig. 2. Schematic of the computational domain, Γ, displaying the mesh discretization. We consider only one quarter of a typical DES cross section with idealized struts (red) impinged upon arterial tissue (blue). The x, y and z directions represent, respectively, the radial, circumferential and axial directions. The half strut separation is L_1, while L_2 represents the half strut thickness. The arterial wall thickness is L. The origin is represented by 0. We refer to the $y-z$ plane as the abluminal-facing plane. (For interpretation of the references to color in this figure legend, the reader is referred to the web version of this article.)

$$\frac{\partial c}{\partial t} + v\frac{\partial c}{\partial x} = D\frac{\partial^2 c}{\partial x^2} + D_1\left(\frac{\partial^2 c}{\partial y^2} + \frac{\partial^2 c}{\partial z^2}\right) - Kc, \quad t > 0, \tag{2.5}$$

$$\frac{\partial c}{\partial x}(0, y, z, t) = 0, \quad (y, z) \in \Gamma_3, \quad t > 0, \tag{2.6}$$

$$c(0, y, z, t) = c_0 \exp\{-\lambda t\}, \quad (y, z) \in \Gamma_1 \cup \Gamma_2, \quad t \geqslant 0, \tag{2.7}$$

$$\frac{\partial c}{\partial y}(x, 0, z, t) = \frac{\partial c}{\partial y}(x, L_1, z, t) = 0, \quad t > 0, \tag{2.8}$$

$$\frac{\partial c}{\partial z}(x, y, 0, t) = \frac{\partial c}{\partial z}(x, y, L_1, t) = 0, \quad t > 0, \tag{2.9}$$

$$c(L, y, z, t) = 0, \quad \forall (y, z), \quad t > 0 \tag{2.10}$$

$$c(x, y, z, 0) = 0 \text{ on } \Gamma \setminus (\Gamma_1 \cup \Gamma_2). \tag{2.11}$$

2.4. One-dimensional model

In the corresponding one-dimensional model we consider only the radial drug transport, with the diffusion coefficient in the radial (x) direction given by D. The model in a Cartesian coordinate system is given by:

$$\frac{\partial c}{\partial t}(x, t) + v\frac{\partial c}{\partial x}(x, t) = D\frac{\partial^2 c}{\partial x^2}(x, t) - Kc(x, t), \quad 0 < x < L, \quad t > 0, \tag{2.12}$$

$$c(0, t) = c_0 \exp\{-\lambda t\}, \quad t \geqslant 0, \tag{2.13}$$

$$c(L, t) = 0, \quad t \geqslant 0, \tag{2.14}$$

$$c(x, 0) = 0, \quad 0 < x < L. \tag{2.15}$$

3. Solution of the models

In this section we outline how the three-dimensional and one-dimensional models are solved. The former is solved numerically while we adopt an analytical approach to solving the latter.

3.1. Numerical solution of the three-dimensional model

We solve Eqs. (2.5), (2.6), (2.8)–(2.11) numerically using the finite volume opensource software openFoam [26]. The computational domain is generated using the openFoam utility blockMesh. Since we model the drug source as an exponentially decaying function of time, rather than modelling drug transport through the stent coating, the radial 'thickness' of the blocks representing the drug filled stent struts was chosen to be sufficiently small so that they could be considered a surface source. In other words, for the purposes of the computation, the stent struts are essentially two-dimensional. Since the strut drug concentration is taken to be uniform in space, the mesh over regions Γ_1 and Γ_2 was chosen to be quite coarse with 8 cells in each of the y and z directions. However, we choose a finer mesh on the abluminal-facing tissue region, Γ_3, consisting of 40 cells in each of the y and z directions. We select an even finer mesh within the arterial wall, with 80 cells in the x direction. A mesh sensitivity study was performed before deciding on this final discretization, which can be seen in Fig. 2. A time-step study was also conducted with time-steps of 0.5, 30, 60, 360 and 3600 s considered. For the chosen mesh, utilizing a time-step of 360 s resulted in less than a 1% difference in the results compared with the 0.5 s time step and so, to reduce computing time, this time-step was chosen for the study. The numerical finite volume schemes used to approximate each of the terms in (2.5) are summarised in Table 2. We refer the reader to the user documentation [26] for full details on the schemes employed. The linear solver used to solve each matrix equation was Preconditioned Bi-Conjugate Gradient (PBiCG) with a Diagonal Incomplete Lower Upper (DILU) preconditioner. The solver tolerance was set to 10^{-9}.

Table 2
Summary of the numerical schemes used.

	Scheme
Time derivative	Crank Nicholson
Gradient	Gauss
Divergence	Gauss limited linear
Laplacian	Gauss linear corrected
Interpolation	Linear

3.2. Analytical solution of the one-dimensional model

We adopt the method of Laplace transformation to solve the model given by Eqs. (2.12)–(2.15). Taking the Laplace transform of (2.12), making use of the initial condition (2.15) and rearranging provides

$$\frac{d^2\bar{c}}{dx^2}(x, s) - \frac{v}{D}\frac{d\bar{c}}{dx}(x, s) - \left(\frac{s + K}{D}\right)\bar{c}(x, s) = 0. \tag{3.1}$$

The general solution of (3.1) is

$$\bar{c}(x, s) = \exp\left\{\frac{v}{2D}x\right\}[A(s)\cosh(m(s)x) + B(s)\sinh(m(s)x)], \tag{3.2}$$

where

$$2m(s) = \sqrt{\left(\frac{v}{D}\right)^2 + \frac{4}{D}(s + K)}.$$

Now, taking Laplace transforms of (2.13) and (2.14) gives rise to

$$\bar{c}(0, t) = \frac{c_0}{s + \lambda}, \tag{3.3}$$

$$\bar{c}(L, t) = 0. \tag{3.4}$$

Applying the conditions (3.3) and (3.4) to (3.2) leads to the solution in Laplace transform space:

$$\bar{c}(x, s) = -\frac{c_0 \exp\left\{\frac{v}{2D}x\right\}\sinh(m(s)(x - L))}{(s + \lambda)\sinh(m(s)L)}. \tag{3.5}$$

Inversion of (3.5) provides the solution. In detail, consider

$$\bar{f}(s) = \frac{\sinh(m(s)(x - L))}{(s + \lambda)\sinh(m(s)L)}. \tag{3.6}$$

Now, the complex inversion formula is

$$f(t) = \frac{1}{2\pi i}\int_{\beta-i\infty}^{\beta+i\infty} \bar{f}(s)\exp\{st\}ds. \tag{3.7}$$

The integrand of (3.7) has a simple pole at $s = -\lambda$ and infinitely many simple poles at the roots of $\sinh(m(s)L) = 0$. By series expansion (or otherwise) it is readily observed that there are no branch points. In practice we evaluate (3.7) using the residue theorem. The residue at the simple pole $s = -\lambda$ is found to be

$$\frac{\sinh\left(\left(\frac{x-L}{2D}\right)\sqrt{v^2 + 4D(K - \lambda)}\right)\exp\{-\lambda t\}}{\sinh\left(\left(\frac{L}{2D}\right)\sqrt{v^2 + 4D(K - \lambda)}\right)}. \tag{3.8}$$

Now, the remaining poles are found by solving

$$\sinh(m(s)L) = 0.$$

Writing the hyperbolic sine function in terms of exponentials, it is readily shown that the poles, s_n, are given by

$$s_n = -\left(\frac{n^2\pi^2 D}{L^2} + \frac{v^2}{4D} + K\right), \quad n = 1, 2, 3, \ldots$$

so that the residue at $s = s_n$ is

$$-\sum_{n=1}^{\infty} \frac{2n\pi D \sin(n\pi x)\exp\left\{-\left(\frac{n^2\pi^2 D}{L^2} + \frac{v^2}{4D} + K\right)t\right\}}{L^2\left(\lambda - \frac{n^2\pi^2 D}{L^2} - \frac{v^2}{4D} - K\right)}. \tag{3.9}$$

Summing the residues gives $f(t)$:

$$f(t) = \frac{\sinh\left(\left(\frac{x-L}{2D}\right)\sqrt{v^2 + 4D(K - \lambda)}\right)\exp\{-\lambda t\}}{\sinh\left(\left(\frac{L}{2D}\right)\sqrt{v^2 + 4D(K - \lambda)}\right)}$$
$$- \sum_{n=1}^{\infty} \frac{2n\pi D \sin(n\pi x)\exp\left\{-\left(\frac{n^2\pi^2 D}{L^2} + \frac{v^2}{4D} + K\right)t\right\}}{L^2\left(\lambda - \frac{n^2\pi^2 D}{L^2} - \frac{v^2}{4D} - K\right)}. \quad (3.10)$$

Returning to (3.5) we see that the solution is given by

$$c(x,t) = -\frac{c_0 \sinh\left(\left(\frac{x-L}{2D}\right)\sqrt{v^2 + 4D(K - \lambda)}\right)\exp\left\{\frac{vx}{2D} - \lambda t\right\}}{\sinh\left(\left(\frac{L}{2D}\right)\sqrt{v^2 + 4D(K - \lambda)}\right)}$$
$$+ \sum_{n=1}^{\infty} \frac{2c_0 n\pi D \sin(n\pi x)\exp\left\{\frac{vx}{2D} - \left(\frac{n^2\pi^2 D}{L^2} + \frac{v^2}{4D} + K\right)t\right\}}{L^2\left(\lambda - \frac{n^2\pi^2 D}{L^2} - \frac{v^2}{4D} - K\right)}.$$
$$(3.11)$$

4. Results

In this section we investigate the uniformity of tissue drug concentration profiles and at the same time compare the results of the one-dimensional model with those of the three-dimensional model. We consider three separate regimes: convection dominated, diffusion dominated and reaction dominated. In addition to the second Damkohler number (as defined in Section 2), we introduce the first Damkohler number, $Da_1 = KL/v$, which compares the relative importance of reaction to convection. The parameter values used for each regime are summarized in Table 3.

4.1. Uniformity of the drug concentrations

We note from Fig. 2 that, due to the geometry under consideration, the two extrema of the drug concentrations in the abluminal-facing $y-z$ plane will be at the origin, 0, (top left vertex) and the point $(0, L_1, L_1)$ (bottom right vertex). It follows that, for all time, the trajectories $P_1(x, 0, 0)$ and $P_2(x, L_1, L_1)$ will represent the maximum and minimum drug concentration trajectories through the arterial wall. Thus, for a given x, the relative difference between the P_1 and P_2 concentrations gives a reasonable approximation of the uniformity of the drug concentration in the $y-z$ plane. In this context, the word "uniformity" should be interpreted loosely as the closeness of the numerical drug concentration values: the more uniform the drug concentrations are then the closer their difference is to zero.

Initially focussing solely on the three-dimensional model, we computed drug concentrations for each of the three regimes for the first 28 days. We found that by 24 h the variation in drug concentration with radial distance had assumed a consistent pattern. That is, beyond 24 h, the profile shape remained the same with only the concentration values reducing with time. Thus, for all of our comparisons, we show concentration profiles only over the first 24 h. Figs. 3–5 display plots of $C(x, 0, 0)$ and $C(x, L_1, L_1)$ for $0 < x < L$ at the times $t = 1, 3, 12$ and 24 h. Also displayed on these plots are the analytical one-dimensional solutions as given by (3.11). In order to quantify the uniformity, we define an appropriate measure, $\|P_1 - P_2\|$, which essentially computes the difference in drug mass per unit area between P_1 and P_2 as calculated from the 3D model, normalized by the drug mass per unit area as calculated from the 1D model (Eq. 3.11):

$$\|P_1 - P_2\| = \frac{\int_0^L c_{3D}(x, 0, 0, t)dx - \int_0^L c_{3D}(x, L_1, L_1, t)dx}{\int_0^L c_{1D}(x, t)dx}.$$

For clarity, the subscripts $3D$ and $1D$ have been included to represent the three-dimensional and one-dimensional solutions, respectively. From a clinical point of view, it is believed that uniform arterial wall drug concentrations are desirable. However, for the purposes of this paper we do not feel it is appropriate to select a uniformity value, that is, a value above which the profiles are deemed not to be uniform and below which the profiles are deemed to be uniform. Instead, we use a combination of graphical illustration and the measure discussed to conceptualize the notion of uniformity.

4.1.1. Convection dominated system

From Fig. 3 (top) we observe that in the convection dominated regime the P_1 and P_2 concentration profiles still differ very slightly at 1 h, but by 3 h are almost identical and remain so for the rest of the period studied. This is backed up by Table 4, where $\|P_1 - P_2\|$ is only 1.4% after one hour, and less than 1% for the remainder of the 24 h, and indeed the remainder of the 28 days studied. Looking more closely at Fig. 3 (top), we see that the region over which P_1 and P_2 noticeably differ extends only one fifth of the way into the arterial wall. Beyond this thickness, uniform profiles are observed within one hour. In Fig. 3 (bottom) we also display tissue concentration profiles within abluminal-facing ($y-z$ plane) slices taken at three different thicknesses and at two different times. The particular (narrow) scale has been chosen to emphasize the differences, but clearer inspection shows that the profiles are highly uniform in all cases. While the profiles may not look uniform on the particular scale chosen, the range of values on each plot show that in fact the profiles are highly uniform in every case. The conclusion is that in this convection dominated system, highly uniform concentration profiles may be achieved quickly throughout the arterial wall, despite the anisotropic nature of the diffusivity.

4.1.2. Diffusion dominated system

From Fig. 4 (top) we observe that in the diffusion dominated regime the concentration profiles along the trajectories P_1 and P_2 track each other closely, although the agreement is not as good as the convection dominated case. After one hour the region over which P_1 and P_2 differ still extends to a depth of approximately 1.5×10^{-4} m into the wall. After 3 h, this region has halved in size to approximately 7.5×10^{-5} m and remains this thickness for the duration of the 28 days studied. However, Table 4 demonstrates that, while the profiles are clearly less uniform than the convection dominated case, the maximum value of $\|P_1 - P_2\|$ is only 4.9% and reduces to 2.8% by hour 3. In Fig. 4 (bottom) we can also see clearly

Table 3
The regimes considered.

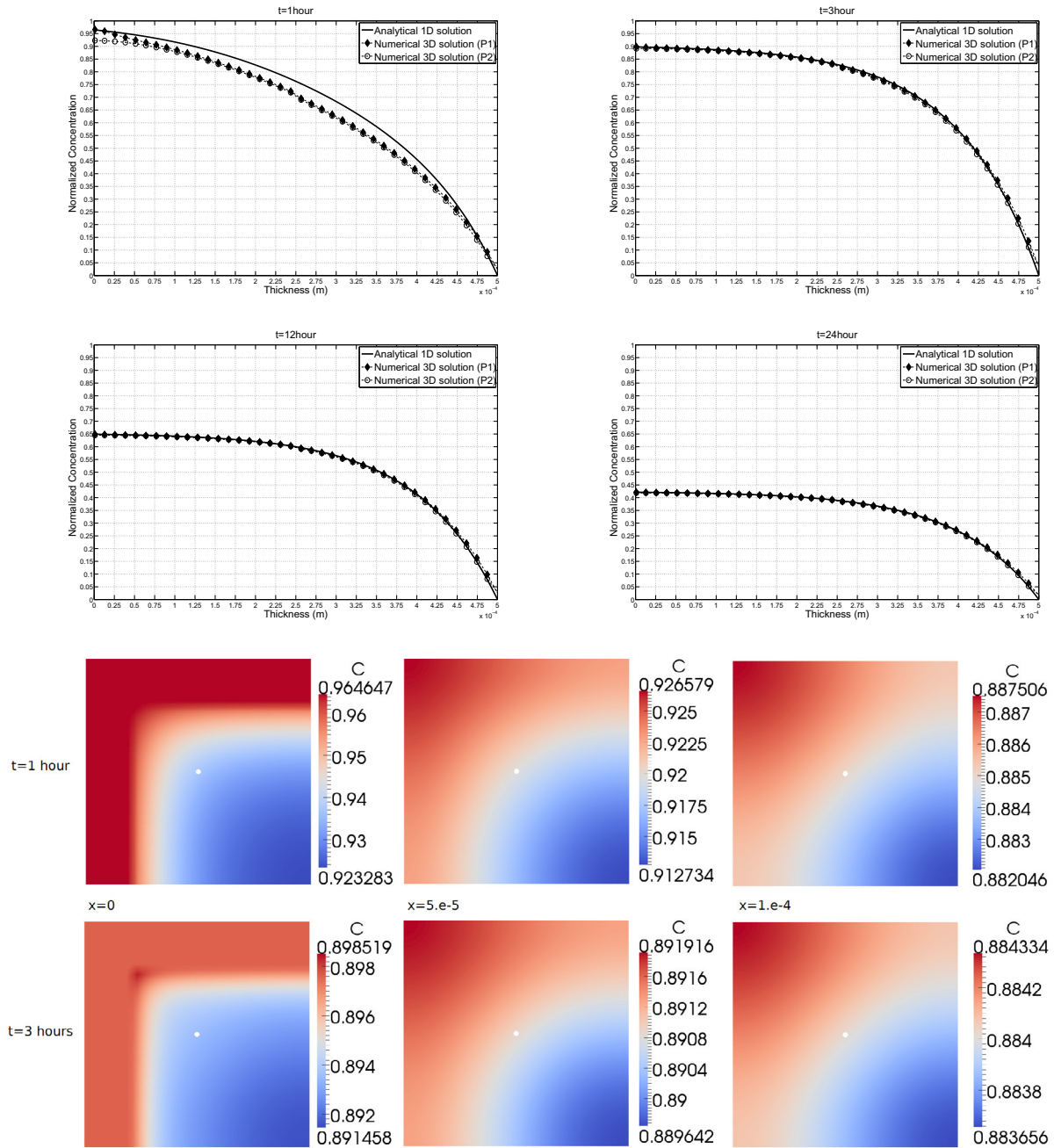| Regime	D_1	D	v	K	Pe	Da_1	Da_2
Convection dominated	10^{-10} m^2 s^{-1}	10^{-11} m^2 s^{-1}	10^{-7} m s^{-1}	10^{-5} s^{-1}	5	0.25	0.05
Diffusion dominated	10^{-10} m^2 s^{-1}	10^{-11} m^2 s^{-1}	10^{-8} m s^{-1}	10^{-5} s^{-1}	0.5	0.25	0.5
Reaction dominated	10^{-10} m^2 s^{-1}	10^{-11} m^2 s^{-1}	10^{-8} m s^{-1}	10^{-4} s^{-1}	0.5	2.5	5

Fig. 3. Convection dominated regime. Top: comparison between numerical (3D) and analytical (1D) concentration profiles at four different times. Bottom: Tissue concentration profiles within abluminal-facing ($y-z$ plane) slices for the convection dominated case. For each time, three slices are taken: $x = 0$ m, $x = 5 \times 10^{-5}$ m and $x = 10^{-4}$ m. These have been chosen since they represent the typical thicknesses across which the profiles are least uniform.

that the range of concentration values is greater in each $y-z$ slice, which indicates less uniform profiles than the convection dominated case. The conclusion here is that in this diffusion dominated system, near uniform concentration profiles can be maintained across the majority of the arterial wall. Close to the lumen, the influence of the strut geometry is most prominent, resulting in a less uniform distribution of drug.

4.1.3. Reaction dominated system

From Fig. 5 (top) we observe that the reaction dominated regime produces the worst levels of uniformity of the three regimes. Similarly to the diffusion dominated case, after one hour the region over which P_1 and P_2 differ still extends to a depth of approximately

1.5×10^{-4} m into the wall and this is maintained for the first 3 h. Even after 24 h and 28 days, P_1 and P_2 still differ across 7.5×10^{-5} m. Despite this, from Table 4 we observe that the maximum $\|P_1 - P_2\|$ is only 6.3% and falls to below 5% by hour 3. In Fig. 5 (bottom) we can see clearly that the range of concentration values is greater in each $y-z$ slice compared with the convection and diffusion dominated cases, which indicates that the profiles are less uniform. Thus the conclusion here is that for this reaction dominated regime, the concentrations feel the effects of the nonuniform stent geometry to a greater degree (and for a longer duration) than the convection and diffusion dominated cases. However, the majority of the arterial wall sees near uniform concentrations for most of the first 24 h and indeed most of the 28 days.
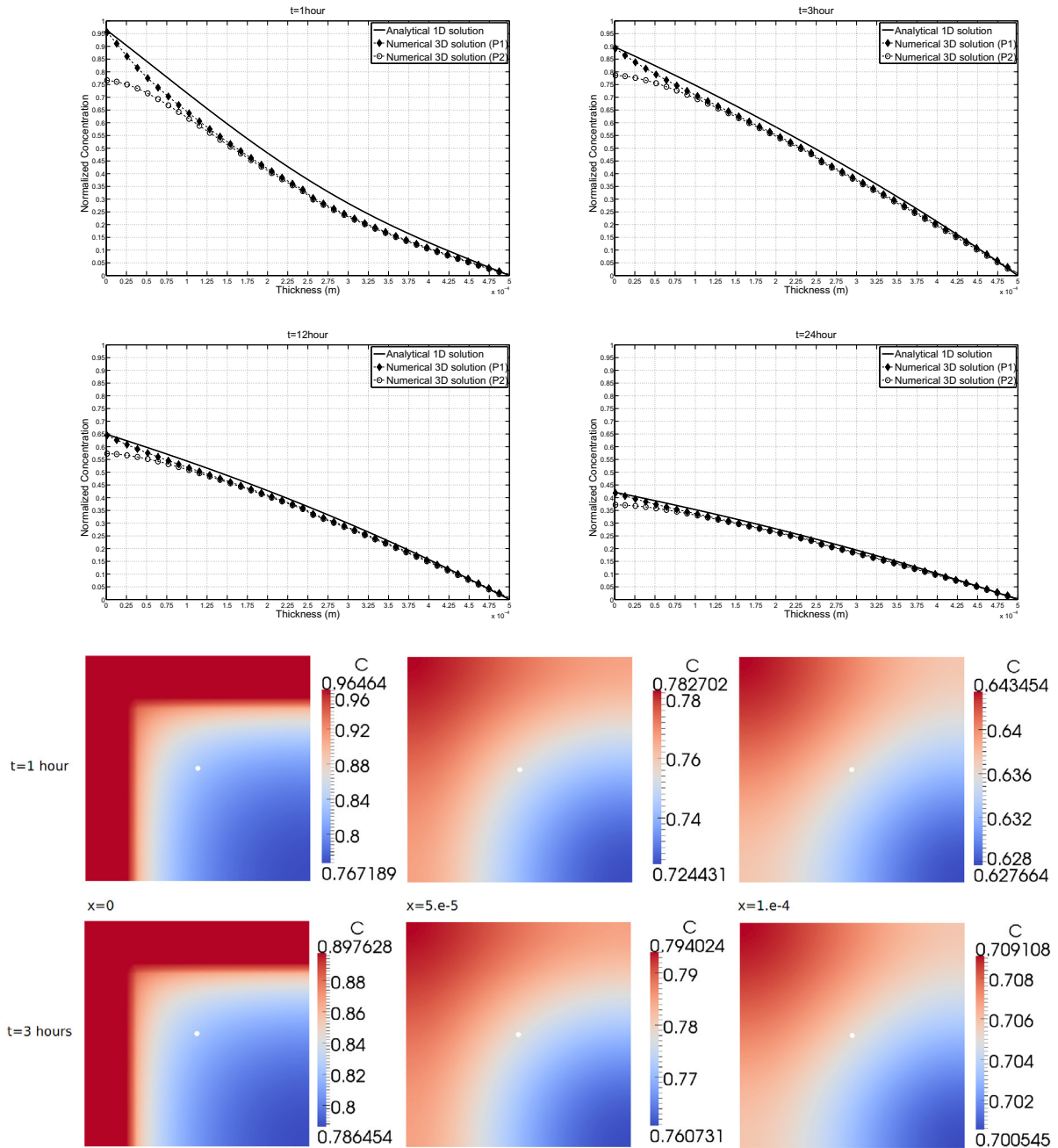
Fig. 4. Diffusion dominated regime. Top: comparison between numerical (3D) and analytical (1D) concentration profiles at four different times. Bottom: tissue concentration profiles within abluminal-facing ($y-z$ plane) slices for the diffusion dominated case. For each time, three slices are taken: $x = 0$ m, $x = 5 \times 10^{-5}$ m and $x = 10^{-4}$ m. These have been chosen since they represent the typical thicknesses across which the profiles are least uniform.

4.2. Comparison between three-dimensional and one-dimensional models

In this section we focus on comparing the results of the one-dimensional and three-dimensional models. Given the demonstration in the previous section of the relatively uniform profiles for each of the regimes, we focus here on the difference between the P_1 three-dimensional solution and the analytical one-dimensional solution as given by (3.11). In order to quantify the difference, we use a similar measure to that used in the previous section. The measure, $\|P_{1_{1D}} - P_{1_{3D}}\|$, essentially calculates the difference in drug mass per unit area between the one-dimensional and three-dimensional models, normalized by

the drug mass per unit area as calculated from the one-dimensional model:

$$\|P_{1_{1D}} - P_{1_{3D}}\| = \frac{\int_0^L c_{1D}(x,t)dx - \int_0^L c_{3D}(x,L_1,L_1,t)dx}{\int_0^L c_{1D}(x,t)dx}.$$

4.2.1. Convection dominated system

In the convection dominated case we see excellent agreement between the one-dimensional and the three-dimensional models (Fig. 3(top)). This is evidenced by the $\|P_{1_{1D}} - P_{1_{3D}}\|$ values in Table 5. After one hour, $\|P_{1_{1D}} - P_{1_{3D}}\|$ is only 5.5% and drops to near
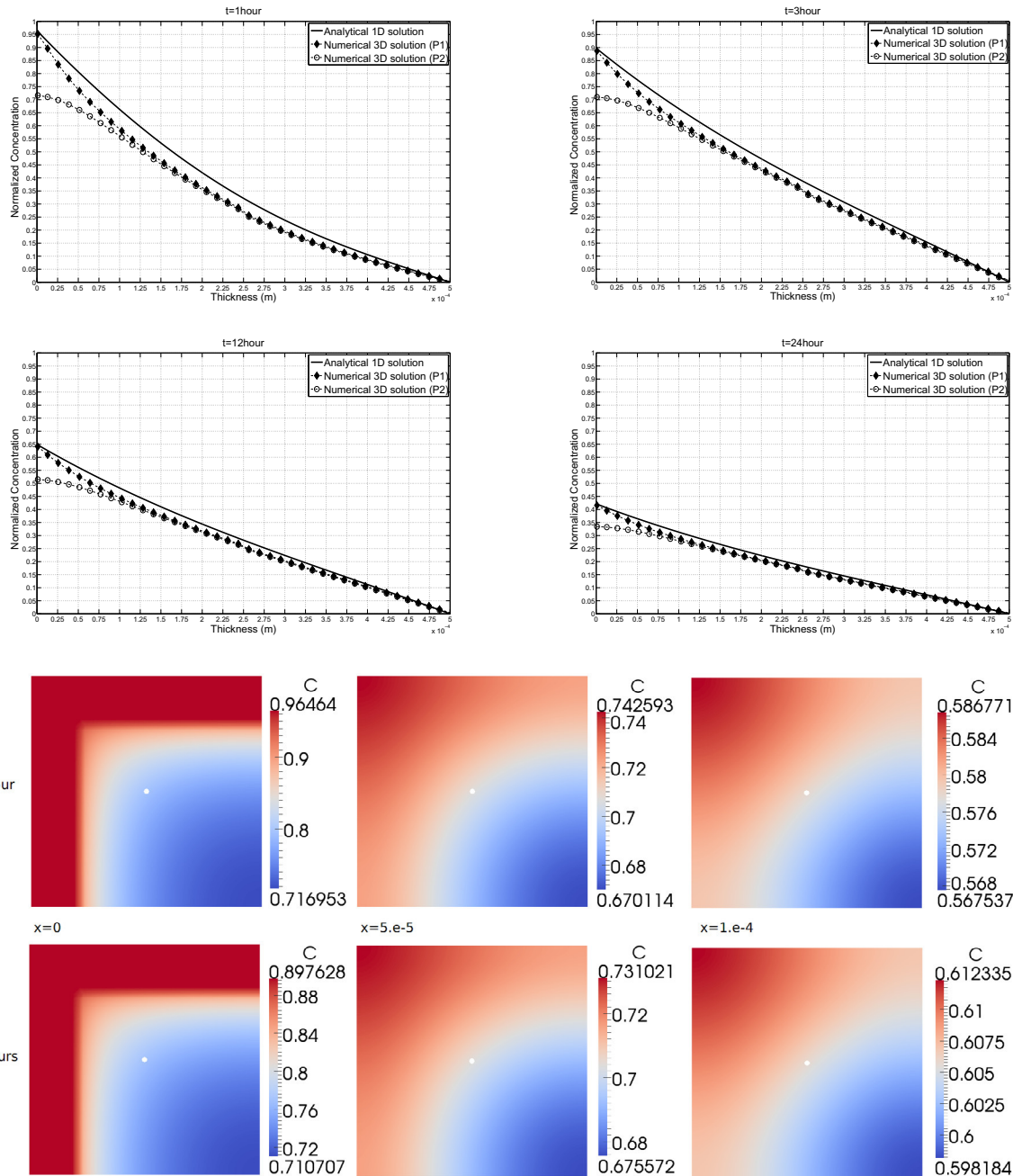
Fig. 5. Reaction dominated regime. Top: comparison between numerical (3D) and analytical (1D) concentration profiles at four different times. Bottom: tissue concentration profiles within abluminal-facing ($y–z$ plane) slices for the reaction dominated case. For each time, three slices are taken: $x = 0$ m, $x = 5 \times 10^{-5}$ m and $x = 10^{-4}$ m. These have been chosen since they represent the typical thicknesses across which the profiles are least uniform.

Table 4
Uniformity $\|P_1 - P_2\|$ for each regime. The lower the percentage value, the greater the uniformity.

Regime	1 h (%)	3 h (%)	12 h (%)	24 h (%)	28 days (%)
	$\|P_1 - P_2\|$				
Convection dominated	1.4	0.8	0.8	0.8	0.8
Diffusion dominated	4.9	2.8	2.7	2.7	2.7
Reaction dominated	6.3	4.6	4.6	4.6	4.6

Table 5
$\|P_{1_{1D}} - P_{1_{3D}}\|$ for each regime. The lower the percentage value, the greater the agreement between the 1D and 3D models.

Regime	1 h (%)	3 h (%)	12 h (%)	24 h (%)	28 days (%)
	$\|P_{1_{1D}} - P_{1_{3D}}\|$				
Convection dominated	5.5	0.1	0.0	0.0	0.0
Diffusion dominated	11.1	5.1	4.2	4.2	4.2
Reaction dominated	11.8	7.6	7.3	7.3	7.3

negligible values by hour 3. Thus in this convection dominated case, the one-dimensional model is adequate at predicting the arterial wall drug distribution.

4.2.2. Diffusion dominated system

In the diffusion dominated regime there is some disagreement between the models at early times (Fig. 4(top) and Table 5) with a $\|P_{1_{1D}} - P_{1_{3D}}\|$ of 11.1% at 1 h. However, by 3 h, the difference is

only 5.1% and falls under 5% for the remainder of the 28 day period. The error in using a one-dimensional model is likely to be within the uncertainty associated with the parameter values.

4.2.3. Reaction dominated system

The reaction dominated regime shows the worst levels of agreement between the one-dimensional and three-dimensional models (Fig. 5 and Table 5), especially at early times. At 1 h, the $\|P_{1_{1D}} - P_{1_{3D}}\|$ is 11.8 %, but by 3 h, this reduces to 7.6%. Even after 24 h, $\|P_{1_{1D}} - P_{1_{3D}}\|$ is still 7.3 % and remains so for the duration of the 28 days studied. Despite this, the one-dimensional model is still providing a reasonable representation of the full three-dimensional model and well within the error tolerances of the parameter values.

4.3. The effect of reducing diffusivity

In this section we examine the effect of reducing the diffusion coefficients on the uniformity of the concentration profiles. Here we maintain the ratio of axial/circumferential to radial diffusion coefficient, i.e. $D_1/D = 10$. We introduce two new regimes where the radial, axial and circumferential diffusion coefficients have all been reduced by a factor of ten. The only two possibilities from our range of parameter values in Table 1 are a new convection dominated regime and a new reaction dominated regime. We find that the effect of decreasing the diffusion coefficients is to reduce the levels of uniformity observed at early times. This is exactly what would be expected since the diffusion timescale in the y and z directions is increased. For the convection dominated case, the $\|P_1 - P_2\|$ value is still 7.9% after 3 h. However, this reduces with time and by 12 h the difference is only 1.1%. However, uniformity is significantly reduced for the reaction dominated case. After 1 h the $\|P_1 - P_2\|$ value is 40.4% and while this reduces, the value is still 12.2% after 24 h. Comparing the one-dimensional model with the three-dimensional model we find that the one-dimensional approximation is good for the convection dominated case in the latter stages of the 24 h period, but not the early stages. For the reaction dominated case, the one-dimensional approximation agrees with P_1 values to within 12.8% by 24 h, but is a poor approximation to the P_2 values. Thus we conclude that the smaller the value of D_1 (with $D_1/D = 10$) the longer it takes for a uniform profile to be achieved. Furthermore, the one-dimensional approximation is less acceptable, especially at predicting concentrations along P_2.

4.4. The effect of increasing anisotropy

We now examine the effect of increasing the anisotropy, i.e. increasing the ratio D_1/D. For the convection and reaction dominated regimes we use the parameter values as the previous section, except that now $D_1 = 10^{-10}$ m^2 s^{-1} so that $D_1/D = 100$. It is not possible to define a diffusion dominated regime with $D_1/D = 100$ that satisfies the range of parameter values in Table 1. However, for completeness we include the diffusion dominated case from Table 3, but increase D_1 to the unrealistic value of $D_1 = 10^{-9}$ m^2 s^{-1}. We find that the effect of increasing the anisotropy is to result in more uniform profiles at earlier times as well as a notable improvement in the comparison between the one-dimensional and three-dimensional solutions.

It is also useful to consider the case where the diffusion coefficient in the axial and circumferential directions are different. We provide one example of this here, making use of the parameter values for the convection dominated case described in the previous section, except that we choose the diffusion coefficients in the mutually perpendicular directions to be an order of magnitude different. Instead of having transversely isotropic diffusion across the y–z plane we now set the diffusion coefficient in the z direction ($D_z = 10^{-10}$ m^2 s^{-1}) to be a factor of ten greater than the diffusion coefficient in the y direction ($D_y = 10^{-11}$ m^2 s^{-1}), which in turn is ten times greater than the diffusion coefficient in the x direction ($D_x = 10^{-12}$ m^2 s^{-1}). As we might have anticipated, this case provides less-uniform profiles and worse agreement between the one-dimensional and three-dimensional models than the corresponding case where $D_z = D_y = D_1 = 100D_x$. However, in this case we would like to emphasize that, due to the loss of symmetry in terms of diffusion across the y–z plane, P_1 and P_2 do not necessarily represent the maximum and minimum drug concentrations in the this plane.

4.5. The effect of varying strut thickness and separation

An interesting question that arises in stent design is what is the optimal thickness and separation of struts? Of course, there are two obvious limitations to this optimization. Firstly, the spacing between the struts must be large enough such that an adequate amount of plasma is exposed to the arterial wall (i.e. a solid cylindrical stent is not an option). Secondly, the thickness of the struts is constrained by mechanical integrity. Over the years, stent designs have been driven towards thinner struts in an attempt to minimize injury (and hence in-stent restenosis). However, whilst a plethora of different geometrical patterns have been used to ensure deliverability and strength (whilst resisting shortening) the effects of such patterns on drug distribution is under-explored. In this section we attempt to partly address this by varying the strut thickness and separation and observing the effect these changes have on the uniformity of the drug concentration and on the comparison between the one-dimensional and three-dimensional models. For our comparison, we keep the amount of drug delivered per cross section of tissue the same, but double the number of struts. The result is that we now have four struts in the same cross section of tissue and the thickness of the struts, $2L_2$, and the strut separation, $2L_1$, are both halved and now take the values L_2 and L_1, respectively. The new configuration is displayed in Fig. 6.

The numerical simulations were performed for the convection dominated, diffusion dominated and reaction dominated cases (Table 3) using the same mesh discretization as the original geometrical configuration. From a comparison between Figs. 3–5(top) with Figs. 7–9 it is evident that the result of reducing the strut thickness and separation is more uniform concentration profiles. This is backed up by the reduction in the $\|P_1 - P_2\|$ values, as displayed in Table 6. Another important effect we observed is the better agreement between the one-dimensional and three-dimensional models when the strut thickness and spacing is reduced. This is clearly visible by comparing Figs. 3–5 with Figs. 7–9 and is also backed up by the reduction in the $\|P_{1_{1D}} - P_{1_{3D}}\|$ values between Tables 5 and 6.

5. Discussion

In this paper we have addressed the validity of two common assumptions that are made in modelling the distribution of drug in the arterial wall following stent-based delivery. Firstly, we have derived two conditions which must be satisfied to allow us to reasonably approximate the curved arterial wall geometry as a rectangular geometry. These conditions depend on the ratio of the arterial wall thickness to the arterial radius, the ratio of arterial wall thickness to strut separation and the ratio of the radial diffusion coefficient to the axial/circumferential diffusion coefficient. This analysis validates the extensive use of this assumption in the literature, at least for the range of parameter values considered
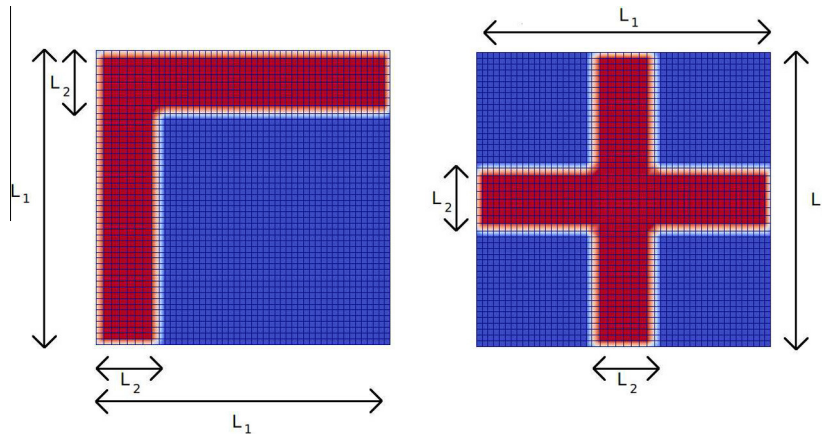
Fig. 6. Comparison between original geometry (left) and geometry with halved strut thickness and separation (right). The cross-sectional area is kept constant.
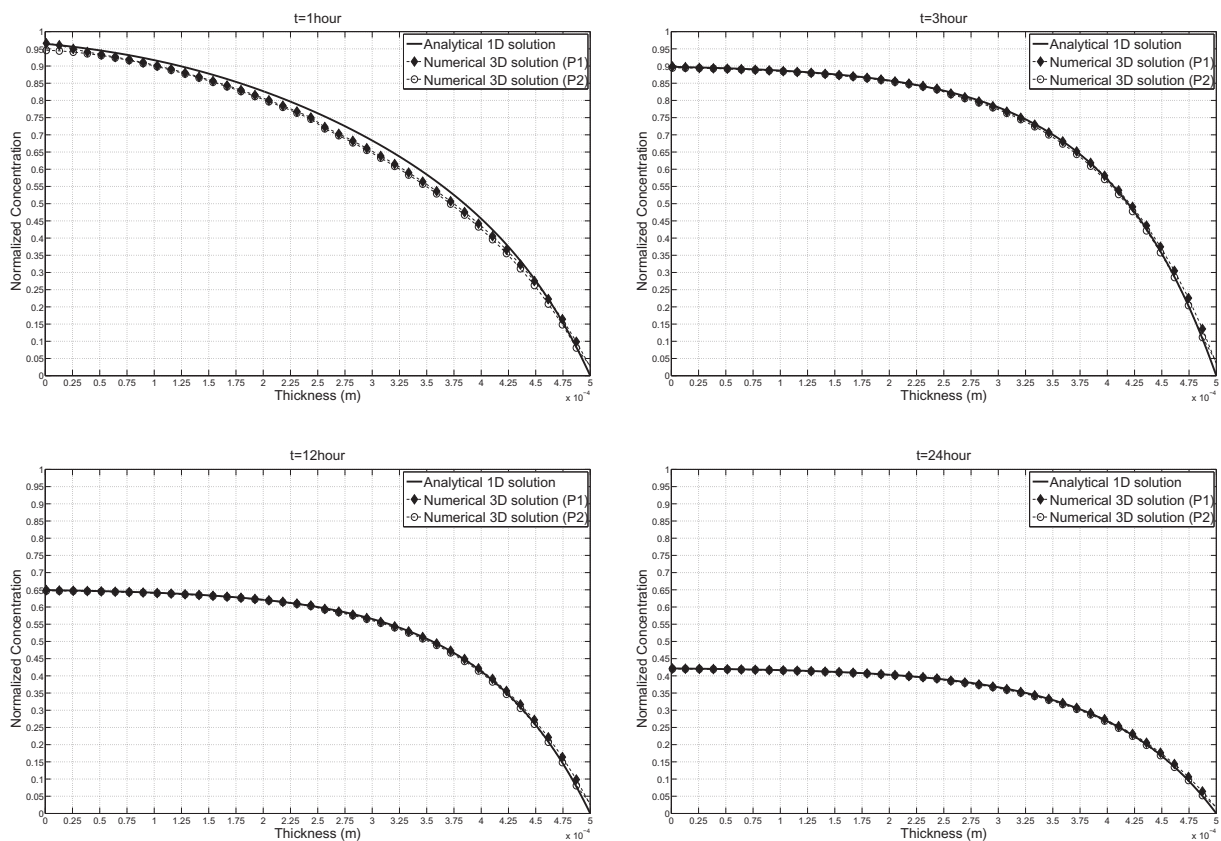

Fig. 7. The case of halved strut thickness and separation. Convection dominated regime.

here. Secondly, by comparing drug transport and distribution predicted by an idealized three-dimensional model with that of a one-dimensional model, we have been able to show that a one-dimensional model is adequate in certain circumstances. Furthermore, we have verified that the anisotropic nature of diffusivity in the arterial wall enhances the agreement between the one-dimensional and three-dimensional models.

We have analysed three distinct regimes within the range of typical parameter values considered. For the convection dominated regime, highly uniform concentration profiles are achieved throughout the arterial wall. This is somewhat surprising since intuition would suggest that the high Peclet radial transport would result in it taking longer for drug to diffuse across the abluminal-facing plane. However, the effect of the radial

uni-directional transmural convection is actually to increase the concentration gradients in the axial and circumferential directions and thus increase the effective diffusivity in this plane. These increased concentration gradients result in uniform concentration profiles in the abluminal-facing plane being obtained more quickly than in the case where radial diffusion dominates over convection. The high radial Peclet number then transmits these uniform concentration profiles throughout the arterial wall. For the diffusion dominated system, transport across the abluminal-facing plane is slower and as such it takes longer for near-uniform profiles to be achieved. Since radial transport is slowed (the timescale for transport across the arterial wall is an order of magnitude slower) the influence of the strut geometry is transmitted a small distance into the arterial wall. When drug absorption is the significant feature,
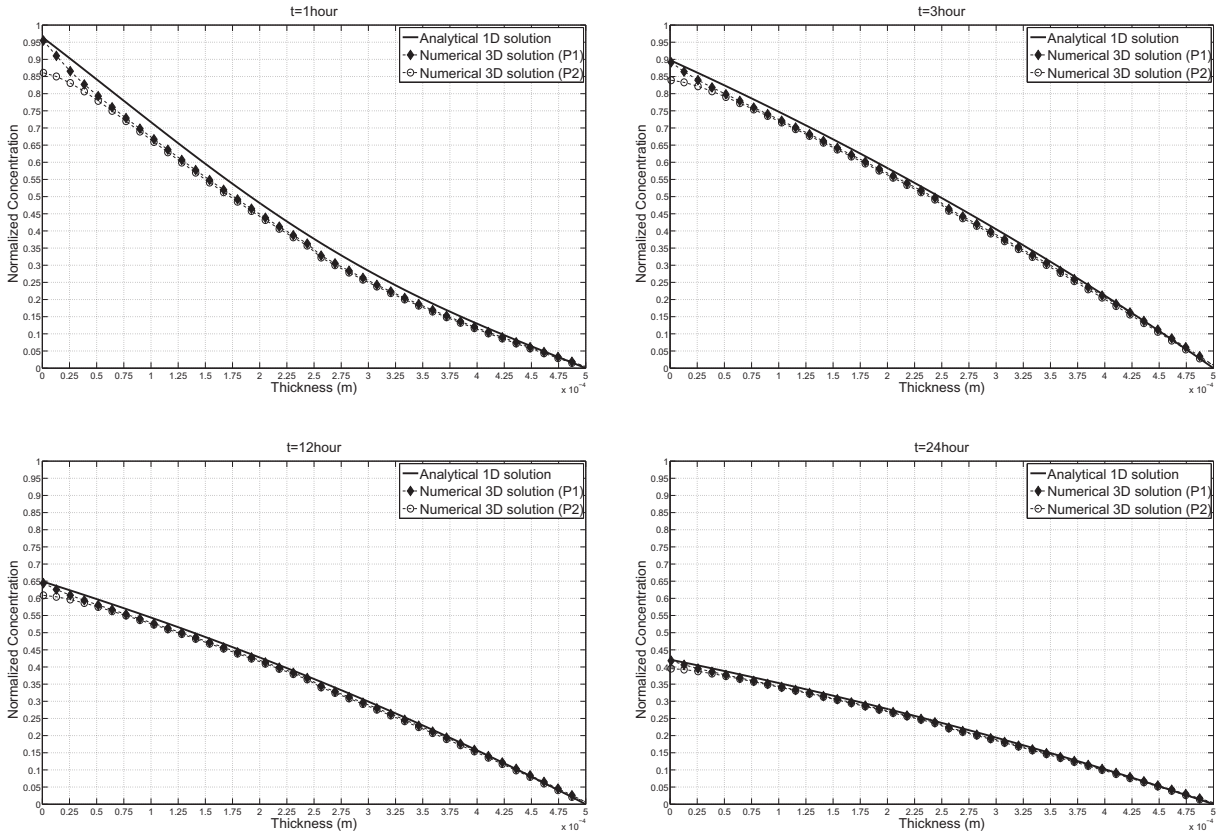
Fig. 8. The case of halved strut thickness and separation. Diffusion dominated regime.
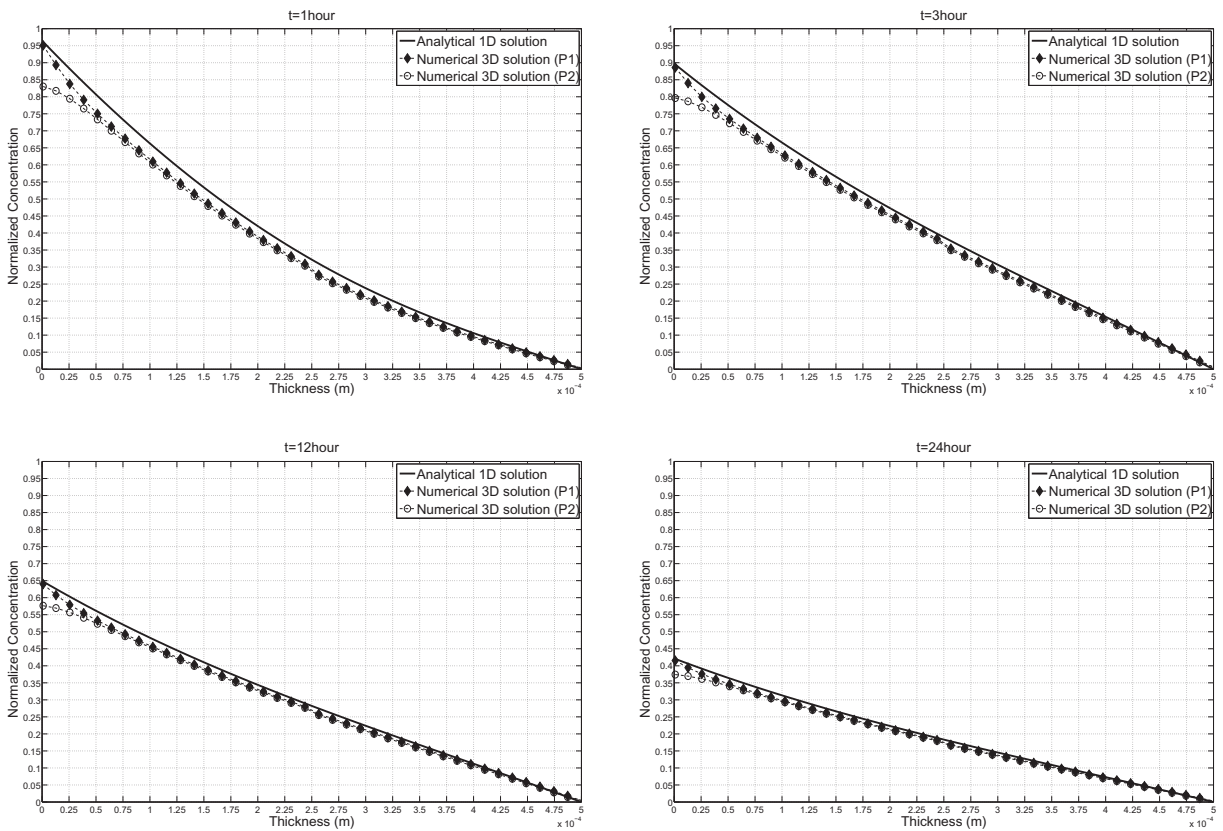

Fig. 9. The case of halved strut thickness and separation. Reaction dominated regime.

Table 6
The case of halved strut thickness and separation. Top: Uniformity $(P_1 - P_2)$ for each regime. The lower the percentage value, the greater the uniformity. Bottom: $(P_{1_{1D}} - P_{1_{3D}})$ for each regime. The lower the percentage value, the greater the agreement between the 1D and 3D models.

Regime	1 h (%)	3 h (%)	12 h (%)	24 h (%)	28 days (%)
$P_1 - P_2$					
Convection dominated	1.0	0.7	0.7	0.7	0.7
Diffusion dominated	2.2	1.5	1.5	1.5	1.5
Reaction dominated	2.7	2.1	2.1	2.1	2.1
$P_{1_{1D}} - P_{1_{3D}}$					
Convection dominated	2.7	0.1	0.1	0.1	0.1
Diffusion dominated	6.8	3.0	2.5	2.5	2.5
Reaction dominated	7.4	4.8	4.6	4.6	4.6

as in the reaction dominated case, the influence of the strut geometry is even more evident. The reason for this lies in the fact that high drug absorption rates reduce the transport of drug through the arterial wall. Despite the less uniform profiles for the diffusion and reaction dominated cases, the majority of the arterial wall sees near uniform profiles for most of the period studied. In all of these cases the one-dimensional model provides a good approximation to the three-dimensional model, especially in the convection dominated case and especially at later times within the first 24 h. Generally speaking, the better the levels of uniformity observed, the better is the one-dimensional model at replicating the results of the three-dimensional model. It is worth emphasizing that the degree of variability of the estimates of the parameters is substantially greater than the difference between the one-dimensional and the three-dimensional model, lending support to the hypothesis that, for the most part, a one-dimensional model provides an adequate description of the diffusion process.

It is interesting to assess our findings in the context of clinical and manufacturing considerations. Clinicians suggest that uniform drug concentration profiles are desirable. If it were the case that drug distribution followed the pattern of the struts then large areas of tissue would be exposed to levels of drug which are ineffective while those areas directly behind the struts may receive toxic levels of drug. From our analysis, we have shown that if uniform profiles were to be required in the early hours of implantation then convection dominated transport would be desired. Since the arterial wall thickness and magnitude of the transmural convection will be fixed for a given patient, the only parameter that can be modified at the manufacturing stage is the drug diffusion coefficient. Thus it appears that low radial drug diffusion coefficients are desirable, giving rise to $Pe > 1$. However, it has been hypothesized that the magnitude of the transmural convection may be a function of disease [24], and actually increases following stent insertion due to the resulting damage to the endothelium. As the endothelium heals, providing greater resistance to transport across the wall, the convection may well decrease resulting in lower Pe values at later times. However, it is anticipated that uniform drug concentrations will be less important at later times when the endothelium has healed since the drug concentrations at these times are likely to be significantly lower than toxic values and therapeutic levels may no longer be required. We have also demonstrated that designing struts that are thinner and closer together results in greater uniformity of drug concentrations more quickly, resulting in better agreement between the one-dimensional and three-dimensional models. Of course there are physiological and mechanical constraints on how close together the struts can be placed and on how thin they can be. Thus there is a balance to be struck between reducing strut thickness and separation to ensure a uniform drug distribution and maintaining mechanical integrity and sufficient tissue exposure to the lumen.

As we have already mentioned, many of the parameters in our model are in fact drug-dependent. Bozsak et al. [15] studied the transport properties of two commercial drugs, paclitaxel and sirolimus, used to coat current drug-eluting stents. They found that due to differences in the diffusion coefficients and binding parameters of these drugs, the main mechanism of transport was different. They found that for paclitaxel the timescale for convection is faster than that for drug binding while for sirolimus the timescale for binding was faster than that for convection. Whilst it should be stressed that [15] considered a more sophisticated model of binding, it is still, nonetheless, interesting to interpret their findings in the context of this present work. If paclitaxel transport through the arterial wall is indeed within the convection dominated regime, then our results suggest that highly uniform drug concentrations may be achieved rapidly throughout the arterial wall for this drug. However, if sirolimus transport through the arterial wall is within the reaction dominated regime then our results suggest less uniform profiles, with the stent strut geometry having an influence on drug distribution close to the lumen. However, in both cases, the majority of the arterial wall would see near-uniform concentration profiles. This would suggest a one-dimensional model may more closely replicate the three-dimensional results of paclitaxel transport through the arterial wall.

Our results have demonstrated that the higher the value of the axial and circumferential diffusion coefficient, D_1, with $D_1/D \geqslant 10$, the quicker the time taken for uniform drug concentrations to be achieved in the abluminal-facing plane, and the better the comparison between the one-dimensional and three-dimensional models. Also, perhaps counter-intuitively, we have demonstrated that the greater the level of anisotropy, i.e. the greater the value of D_1/D, the more uniform the drug concentrations are and the better the comparison between the one-dimensional and three-dimensional models.

In summary, the ideal situation from a drug delivery point of view would appear to be the manufacturing of a device with thin struts that are close together, containing a drug that possesses fast circumferential and axial diffusion coefficients which are much larger than the radial diffusion coefficient $(D_1/D \gg 1)$, and satisfy $Pe > 1$. Under these conditions, uniform drug concentrations are achieved quickly and are transmitted through the arterial wall. In this case the one-dimensional model best replicates the three-dimensional model. In contrast, the least ideal situation from a clinical point of view would appear to be the manufacturing of a device with thick struts that are far apart and contain a drug that possesses slow circumferential and axial diffusion coefficients of the same order as the radial diffusion coefficient and satisfying $Da_1 > 1$ and $Da_2 > 1$. Under these conditions, uniform drug concentrations are not achieved throughout the wall and this could result in regions of toxicity and/or regions of under-exposure to therapeutic levels of drug. A non-negligible area of highly non-uniform drug concentrations persists close to the lumen even after 24 h. For these reasons, in this case the one-dimensional model is a poor representation of the three-dimensional model.

6. Limitations and applicability

We believe that it is appropriate to reiterate that a number of simplifications have been made in this analysis. Firstly, we do not model the release of drug from the device but instead assume that the drug concentration may be described by an exponentially decaying function of time with a prescribed release rate. Secondly, we model the arterial wall as a single layer with diffusion coefficients, convection and reaction parameters that are independent of space, concentration and time. Our justification for neglecting the intima layer of the wall (closest to the lumen) is that it is likely

to be severely damaged or removed during the stent expansion process and we neglect the adventitia since we have previously demonstrated that the presence of the adventitia has little effect on the observed drug concentrations in the media where the drug is targeted [24]. We choose our boundary conditions in such a way that drug cannot be lost to the flowing blood in the lumen. This may be justified by the fact that stents are now routinely coated abluminally to reduce washout.

We also acknowledge that we do not fully model the binding of drug to components within the arterial wall, since the focus of this work is to study the effect of anisotropic diffusion on the uniformity of drug distribution, and to make comparisons between one-dimensional analytical and three-dimensional numerical solutions. Several models of drug binding have been proposed in the literature, but the most appropriate model for a given system may well depend on the particular drug considered. Instead, for the purpose of this study we assume that drug is absorbed at a prescribed rate. The absorption model we consider can be shown to be a special case of the most complex non-linear saturable binding model that has been proposed for drug binding in the arterial wall. Specifically, at early times (up to around 1 day), the non-linear model is well approximated by the linear absorption model. After this time, when the drug binding sites have become saturated, then the transport process will be heavily influenced by the unbinding rate: if this is sufficiently small then we may revert to either diffusion or convection dominated transport.

Perhaps the most significant assumption is that the arterial geometry is that of a rigid cylinder. In reality, this is not the case, especially when there exists significant levels of disease. However, to date most of the modelling in this field assumes an idealized geometry, as we have here. It is likely that some of the effects observed in this study may be replicated in more realistic patient-specific geometries, at least under certain circumstances. We would like to reiterate that the analysis applied here is not specific to drug-eluting stents, nor drug distribution in arterial tissue. For example, many of the ideas and conclusions presented in this paper may be applied to arterial drug distribution following delivery from drug coated balloons. Of course, the geometrical configuration would differ from that presented in Fig. 1 and the exponentially decaying boundary condition would require modification.

Conflict of interest

None declared.

Acknowledgments

References

[1] S. McGinty, A decade of modelling drug release from arterial stents, Math. Biosci. 257 (2014) 80–90.

[2] J.R. Stark, J.M. Gorman, E.M. Sparrow, J.P. Abraham, R.E. Kohler, Controlling the rate of penetration of a therapeutic drug into the wall of an artery by means of a pressurized balloon, J. Biomed. Sci. Eng. 6 (2013) 527–532.

[3] J.P. Abraham, J.R. Stark, J.M. Gorman, E.M. Sparrow, R.E. Kohler, A model of drug deposition within artery walls, J. Med. Device 7 (2013) 020902.

[4] A.R.A. Khaled, K. Vafai, The role of porous media in modeling flow and heat transfer in biological tissues, Int. J. Heat Mass Transfer 46 (2003) 4989–5003.

[5] A. Quezada, K. Vafai, Modeling and analysis of transport in the mammary glands, Phys. Biol. 11 (2014). 045004 (18pp).

[6] G. Pontrelli, F. de Monte, A multi-layer porous wall model for coronary drug-eluting stents, Int. J. Heat Mass Transfer 53 (1) (2010) 3629–3637.

[7] A.R. Tzafriri, A. Groothuis, G. Sylvester Price, E.R. Edelman, Stent elution rate determines drug deposition and receptor-mediated effects, J. Controlled Release 161 (2012) 918–926.

[8] X. Zhu, D.W. Pack, R.D. Braatz, Modelling intravascular delivery from drug-eluting stents with biodurable coating: investigation of anisotropic vascular drug diffusivity and arterial drug distribution, Comput. Methods Biomech. Biomed. Eng. 17 (3) (2012) 1–12.

[9] G. Pontrelli, F. de Monte, Mass diffusion through two-layer porous media: an application to the drug-eluting stent, Int. J. Heat Mass Transfer 50 (17–18) (2007) 3658–3669.

[10] G. Pontrelli, F. de Monte, Modelling of mass dynamics in arterial drug-eluting stents, J. Porous Media 12 (1) (2010) 19–28.

[11] S. McGinty, S. McKee, R.M. Wadsworth, C. McCormick, Modeling arterial wall drug concentrations following the insertion of a drug-eluting stent, SIAM J. Appl. Math. 73 (6) (2013) 2004–2028.

[12] J.P. Abraham, J.M. Gorman, E.M. Sparrow, J.R. Stark, R.E. Kohler, A mass transfer model of temporal drug deposition in artery walls, Int. J. Heat Mass Transfer 58 (1–2) (2013) 632–638.

[13] C.W. Hwang, D. Wu, E.R. Edelman, Physiological transport forces govern drug-distribution for stent based delivery, Circulation 104 (7) (2001) 600–605.

[14] A.D. Levin, N. Vukmirovic, C.W. Hwang, E.R. Edelman, Specific binding to intracellular proteins determines arterial transport properties for rapamycin and paclitaxel, Proc. Natl. Acad. Sci. USA 101 (25) (2004) 9463–9467.

[15] F. Bozsak, J.M. Chomaz, A.I. Barakat, Modeling transport of drugs eluted from stents: physical phenomena driving drug distribution in the arterial wall, Biomech. Model. Mechanobiol. 13 (2) (2014) 327–347.

[16] W.J. Denny, M.T. Walsh, Numerical modelling of mass transport in an arterial wall with anisotropic transport properties, J. Biomech. 47 (2014) 168–177.

[17] J.M. Weiler, E.M. Sparrow, R. Ramazani, Mass transfer by advection and diffusion from a drug-eluting stent, Int. J. Heat Mass Transfer 55 (2012) 1–7.

[18] R. Mongrain, I. Faik, R. Leask, J. Rodes-Cabau, E. Larose, O. Bertrand, Effects of diffusion coefficients and struts apposition using numerical simulations for drug eluting coronary stents, J. Biomech. Eng. 129 (2007) 733–742.

[19] P. Zunino, C. D'Angelo, L. Petrini, C. Vergara, C. Capelli, F. Migliavacca, Numerical simulation of drug eluting coronary stents: mechanics, fluid dynamics and drug release, Comput. Methods Appl. Mech. Eng. 198 (2009) 3633–3644.

[20] G. Vairo, M. Cioffi, R. Cottone, G. Dubini, F. Migliavacca, Drug release from coronary artery stents: a multidomain approach, J. Biomech. 43 (2010) 1580–1589.

[21] M. Horner, S. Joshi, V. Dhruva, S. Sett, S.F.C. Stewart, A two-species drug delivery model is required to predict deposition from drug-eluting stents, Cardiovasc. Eng. Technol. 1 (3) (2010) 225–234.

[22] D.M. Saylor, J.E. Soneson, J.J. Kleinedler, M. Horner, J.A. Warren, A structure-sensitive continuum model of arterial drug deposition, Int. J. Heat Mass Transfer 82 (2015) 468–478.

[23] L. Ai, K. Vafai, PA coupling model for macromolecules transport in a stenosed arterial wall, Int. J. Heat Mass Transfer 49 (2006) 1568–1591.

[24] S. McGinty, S. McKee, R.M. Wadsworth, C. McCormick, Modelling drug-eluting stents, Math. Med. Biol. 28 (2010) 1–29.

[25] S. McGinty, Stents and arterial flows (Ph.D. Thesis), University of Strathclyde, United Kingdom, 2010.

[26] The OpenFoam Foundation. 2011–2014. See <http://www.openfoam.org>.